



Stony Brook University

Precise Measurement of the Neutron Skin Thicknesses of ^{208}Pb and ^{48}Ca

Dissertation Defense

Weibin Zhang

Department of Physics and Astronomy
Stony Brook University

February 2, 2023

Defence Committee:

James Lattimer, Jiangyong Jia, Ciprian Gal

Advisor:

Abhay Deshpande

Introduction

Experimental Setup

Data Analysis

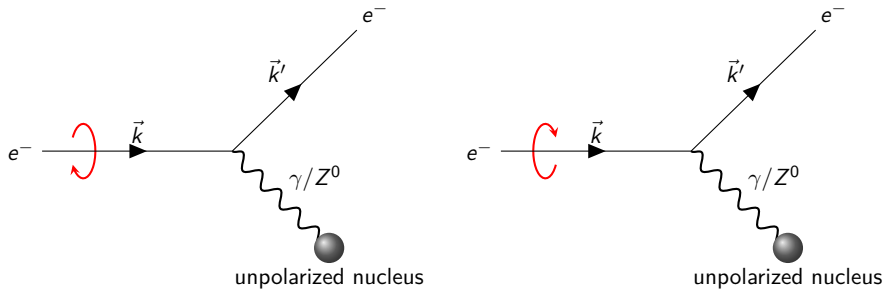
Systematic Uncertainties

Result and Discussion

Transverse Asymmetry

Introduction

Overview



- PREX-II and CREX are high-precision measurements of the neutron skin thicknesses of ^{208}Pb and ^{48}Ca
- $\mathcal{A}_{\text{PV}} = \frac{\sigma^{\rightarrow} - \sigma^{\leftarrow}}{\sigma^{\rightarrow} + \sigma^{\leftarrow}} \sim \text{ppm}$, $\frac{\delta \mathcal{A}}{\mathcal{A}} \lesssim 4\% \Rightarrow \delta R_n \lesssim 0.05 \text{ fm}$

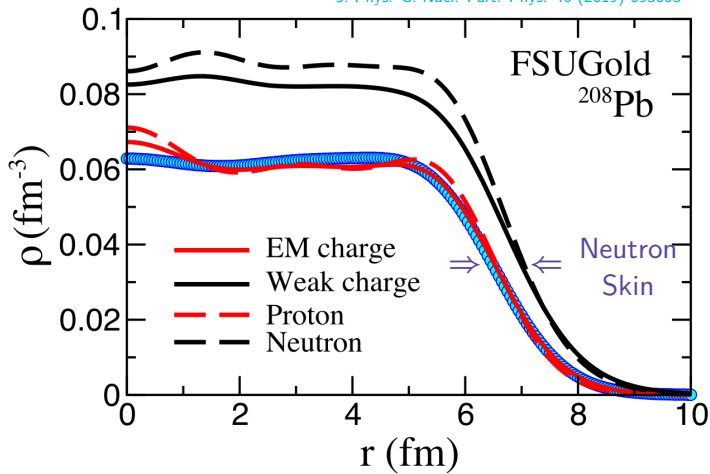
Motivations

Study fundamental nuclear structure: what is the size of a nucleus? How are neutrons distributed in nuclei?

- Test microscopic models: bridge ab-initio methods and the nuclear Density Functional Theory (DFT)
- Constrain three-nucleon force in ab-initio methods and isovector ($\rho_n - \rho_p$) contribution in DFT
- Determine the symmetry energy (J) and its density dependence (L) at the nuclear saturation density ($\rho_0 \sim 0.15 \text{ fm}^{-3}$)
- Infer size and the direct Urca process threshold density of neutron stars
- etc.

Neutron Skin Thickness

J. Phys. G: Nucl. Part. Phys. 46 (2019) 093003



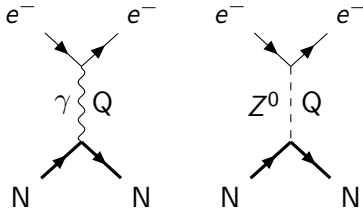
$$R_{p,n} \equiv \langle R_{p,n}^2 \rangle^{1/2} = \sqrt{\frac{\int d^3r \rho_{p,n}(r) r^2}{\int d^3r \rho_{p,n}(r)}} \quad R_{\text{skin}} \equiv R_n - R_p$$

Parity-Violating Electron Scattering (PVES)

- Weak probe
- Interference with EM amplitude
- Clean, no QCD background as in hadronic probes
- Asymmetry is sensitive to the neutron distribution

	Electric charge	Weak charge
Proton	1	0.07
Neutron	0	-0.99

Asymmetry



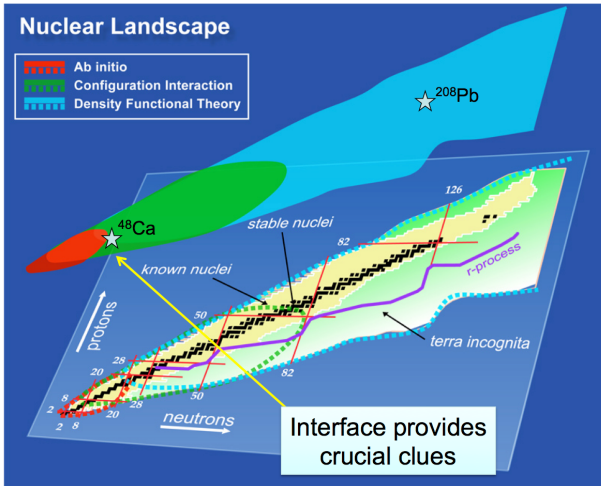
- γ interacts with only vector current
- Z^0 interacts with both vector and axial-vector currents

$$\mathcal{A}_{PV} = \frac{\left(\frac{d\sigma}{d\Omega}\right)^R - \left(\frac{d\sigma}{d\Omega}\right)^L}{\left(\frac{d\sigma}{d\Omega}\right)^R + \left(\frac{d\sigma}{d\Omega}\right)^L} \approx \frac{G_F Q^2}{4\pi\alpha\sqrt{2}} \frac{Q_{wk}}{Z} \frac{F_{wk}(Q^2)}{F_{ch}(Q^2)} \sim 10^{-4} \frac{Q^2}{\text{GeV}^2}$$

where:

$$F(Q^2) = \int d^3r \frac{\sin(Qr)}{Qr} \rho(r)$$

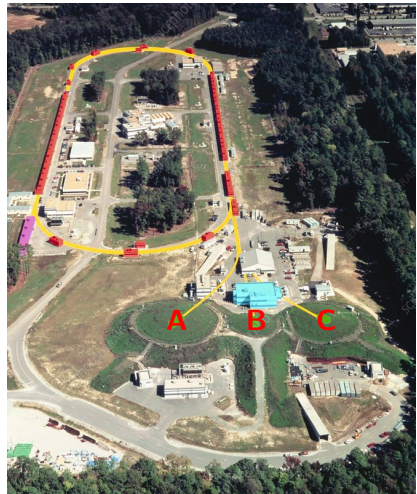
Why ^{208}Pb and ^{48}Ca ?



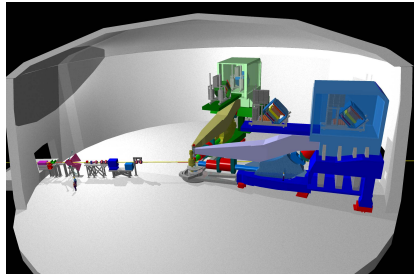
- Doubly magic nuclei
- Spin-0

Experimental Setup

Hall A at JLab



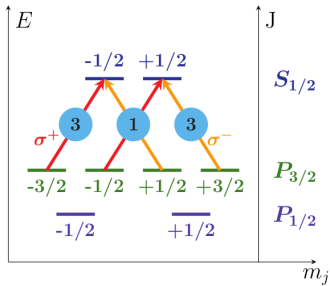
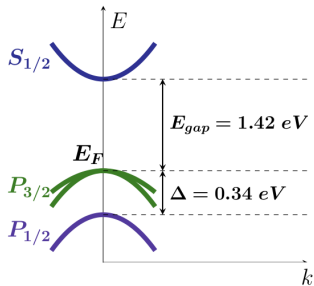
CEBAF



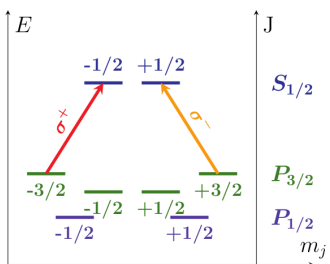
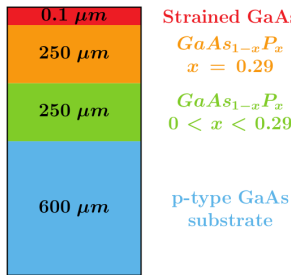
Hall A

	PREX-II	CREX
E (GeV)	0.95	2.18
θ (deg)	4.7	4.5

Polarized Electron Source: GaAs-Based Semiconductor

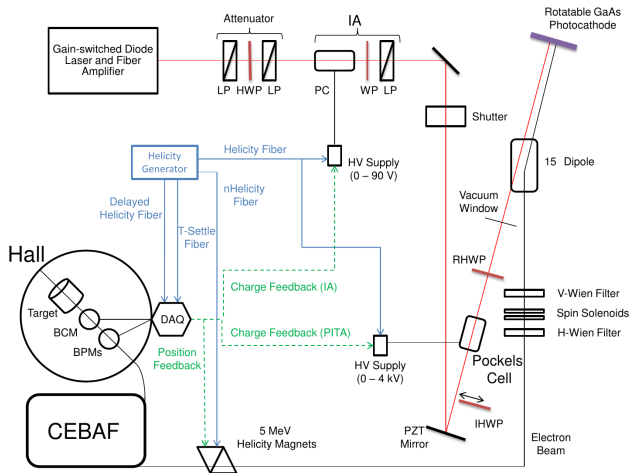


$$\mathcal{P} = \frac{3-1}{3+1} = 50\%$$



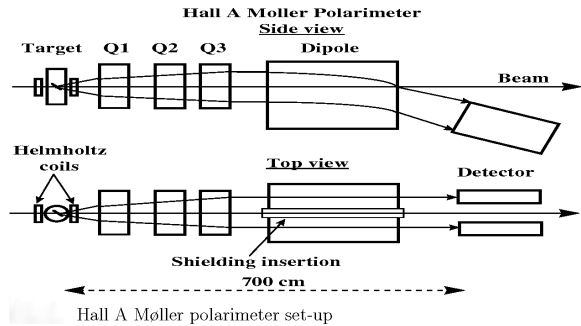
$$\mathcal{P} = 100\%$$

Helicity Control

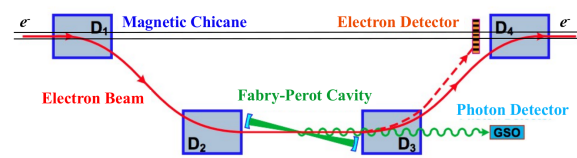


- Pockels Cell (PC): fast helicity flipping
- Insertable Half-Wave Plate (IHWP): slow helicity flipping
- Wien Filter: very slow helicity flipping

Polarimeters

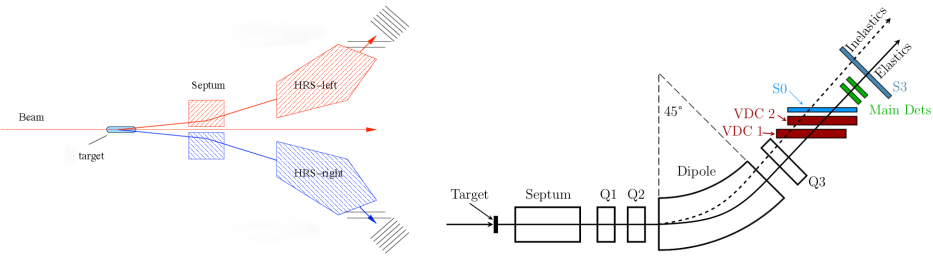


- Invasive, happens every few days
- PREX-II:
 $\mathcal{P} = (89.67 \pm 0.80)\%$
- CREX:
 $\mathcal{P} = (87.06 \pm 0.74)\%$



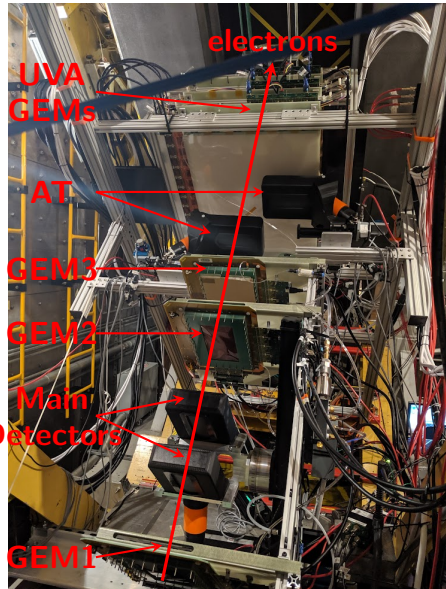
- Non-invasive
- PREX-II:
 $\mathcal{P} = (89.68 \pm 0.15)\%$
- CREX:
 $\mathcal{P} = (87.115 \pm 0.453)\%$

Septum and HRS



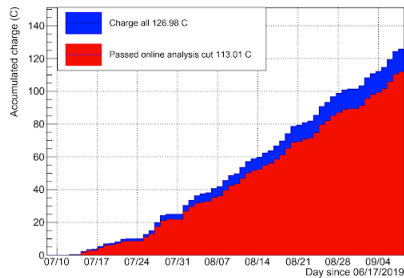
- Septum: make the small scattering angle of $\sim 5^\circ$ possible
- High Resolution Spectrometer (HRS): precise Q^2 measurement, reject inelastic scatterings

Detectors

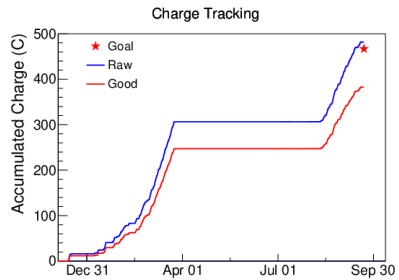


- Main Detectors: 5 mm thick fused silica (quartz) with a size of 16 cm long by 3.5 cm wide
- AT: also a quartz detector, used for monitoring the transverse polarization
- GEM: for optics study

Run Time



PREX-II: Jul - Sep, 2019



CREX: Dec, 2019 - Mar, 2020
Aug - Sep, 2020

Data Analysis

Asymmetry Extraction and Interpretation

$$\mathcal{A}_{\text{cor}} = \mathcal{A}_{\text{raw}} - \sum_i \beta_i \Delta x_i$$

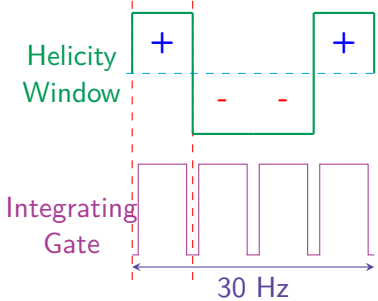
$$\mathcal{A}_{\text{PV}} = \frac{\mathcal{A}_{\text{cor}}/\mathcal{P} - \sum_i \mathcal{A}_i f_i}{1 - \sum_i f_i}$$

$$\langle \mathcal{A} \rangle = \frac{\int d\theta \sin \theta \mathcal{A}(\theta) \frac{d\sigma}{d\Omega} \epsilon(\theta)}{\int d\theta \sin \theta \frac{d\sigma}{d\Omega} \epsilon(\theta)}$$

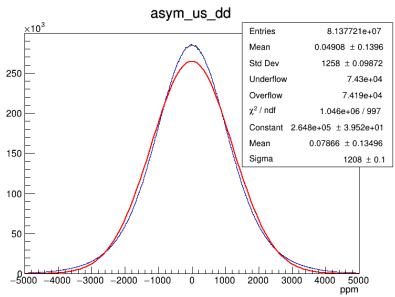
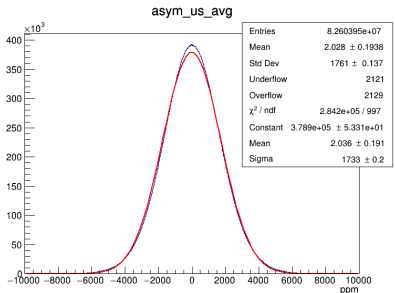
- \mathcal{A}_{cor} : corrected asymmetry
- \mathcal{A}_{raw} : raw asymmetry
- β_i : correction coefficient
- Δx_i : beam fluctuation
- \mathcal{P} : beam polarization
- \mathcal{A}_i : background asymmetry
- f_i : background fraction

- $\mathcal{A}(\theta)$: theoretical prediction
- $\epsilon(\theta)$: acceptance function

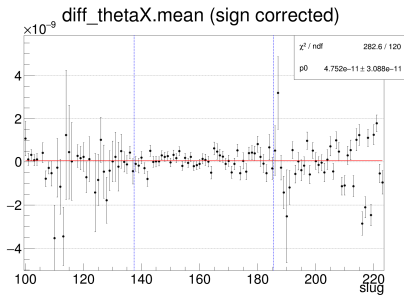
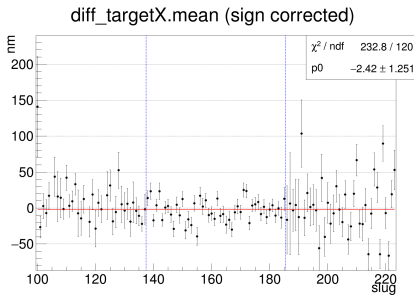
Raw Data (\mathcal{A}_{raw})



$$\begin{aligned}
 \mathcal{A}_{\text{raw}} &= \frac{n^+ - n^-}{n^+ + n^-} + \mathcal{A}_{\text{blind}} \\
 &\approx \frac{N^+ - N^-}{N^+ + N^-} - \frac{I^+ - I^-}{I^+ + I^-} + \mathcal{A}_{\text{blind}}
 \end{aligned}$$



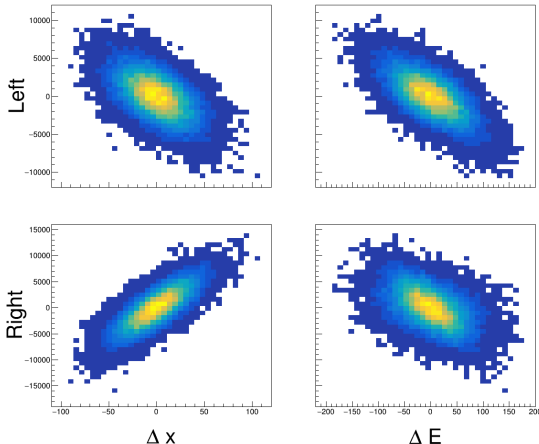
Helicity Correlated Beam Asymmetry (HCBA)



- False asymmetry caused by beam fluctuations
- Though of the fast helicity reversal, there is no way to eliminate beam fluctuations completely

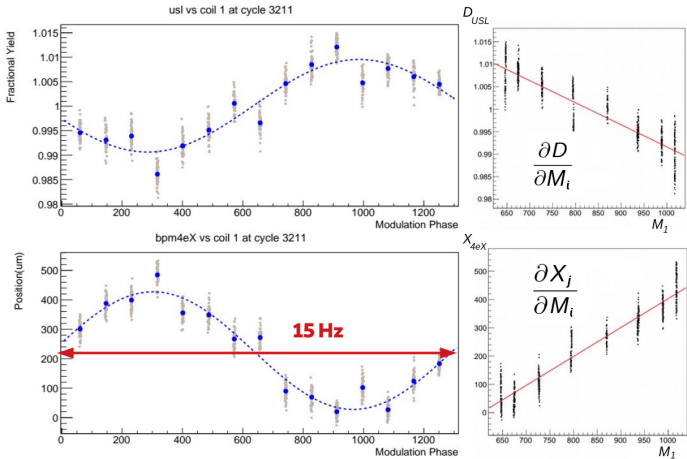
Regression

$$\mathcal{A}_{\text{cor}} = \mathcal{A}_{\text{raw}} - \sum_i \beta_i \Delta x_i$$



- Based on natural beam fluctuations, minimize the χ^2 of a given fit: $\chi^2 = \sum_i \left(\mathcal{A}_{\text{raw}} - \sum_i \beta_i \Delta M_i \right)^2 \quad \frac{\partial \chi^2}{\partial \beta_i} = 0$

Beam Modulation $\mathcal{A}_{\text{cor}} = \mathcal{A}_{\text{raw}} - \sum_i \beta_i \Delta x_i$



- Modulate the beam deliberately, and then measure the detector (monitor) response: $\frac{\partial D}{\partial C_j} = \sum_i \beta_i \frac{\partial M_i}{\partial C_j}$ $\beta_i = \frac{\partial D}{\partial M_i}$

Lagrangian Multiplier

$$\mathcal{A}_{\text{cor}} = \mathcal{A}_{\text{raw}} - \sum_i \beta_i \Delta x_i$$

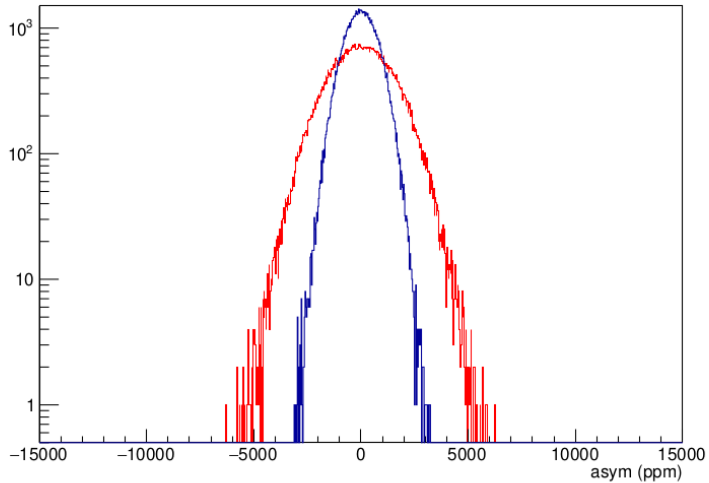
$$\mathcal{L} = \chi^2 + \sum_i \lambda_i \left(\sum_j \frac{\partial D}{\partial C_j} \frac{\partial C_j}{\partial M_i} - \frac{\partial D}{\partial M_i} \right)$$

$$\frac{\partial \mathcal{L}}{\partial \beta} = 0 \quad \frac{\partial \mathcal{L}}{\partial \lambda} = 0$$

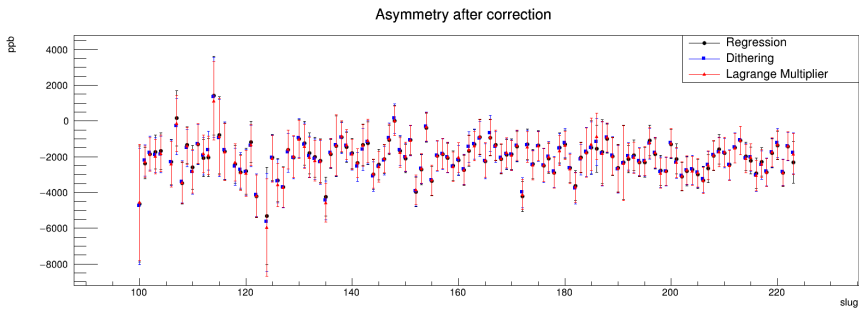
- Regression is susceptible to instrumental noise
- Dithering is accurate, but not precise, limited by the low modulation frequency
- Lagrangian multiplier: try to combine these 2 techniques to avoid their drawbacks, while keeping their advantages

Corrected Asymmetry (\mathcal{A}_{cor})

Ap, Raw (red) vs. Corrected (blue)



Comparison Between the Three Methods



- Good agreement between the three methods
- Asymmetries corrected with the Lagrangian Multiplier are used

Systematic Uncertainties

Carbon Contamination in Pb Target

$$\mathcal{A}_{\text{PV}} = \frac{\mathcal{A}_{\text{cor}}/\mathcal{P} - \sum_i \mathcal{A}_i \mathbf{f}_i}{1 - \sum_i \mathbf{f}_i}$$

Why D-Pb-D sandwich target?

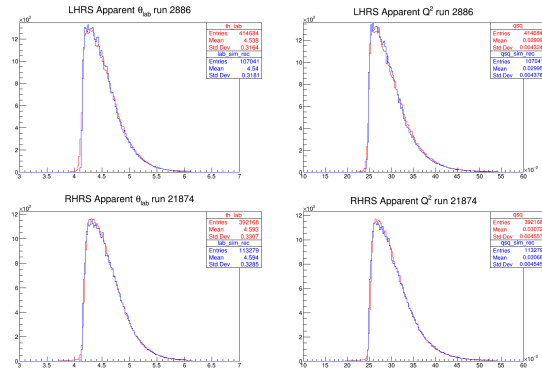
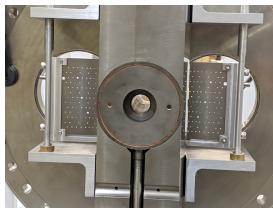
- Lead has low melting point, and low thermal conductivity
- Diamond foils have excellent thermal conductivity
- Carbon background is clean
- The largest dilution: $f_c = (6.3 \pm 0.5)\%$
- Asymmetry correction: $\Delta\mathcal{A} = (0.7 \pm 1.4)$ ppb

Acceptance Function

$$\langle \mathcal{A} \rangle = \frac{\int d\theta \sin \theta \mathcal{A}(\theta) \frac{d\sigma}{d\Omega} \epsilon(\theta)}{\int d\theta \sin \theta \frac{d\sigma}{d\Omega} \epsilon(\theta)}$$

- The PREX-II/CREX experiments measure the average asymmetry over the spectrometer scattering angle acceptance
- An acceptance function is needed to connect our measurement with theoretical models
- The acceptance function is extracted from simulations

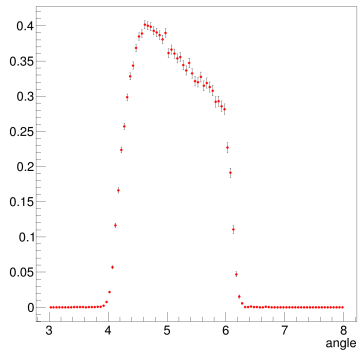
CREX Acceptance Function: How Do We Know the Simulation is Correct



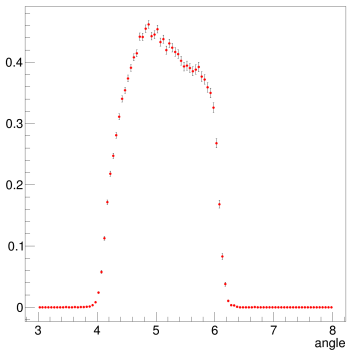
- There are sieve planes in front of the septum for track reconstruction
- By scanning through different parameters, we can identify the best model

CREX Acceptance Function: Result

LHRS acceptance function



RHRS acceptance function



- LHRS (RHRS): Left (Right)-HRS
- The acceptance functions between the two arms are not exactly the same

Result and Discussion

Final Number: \mathcal{A}_{PV}

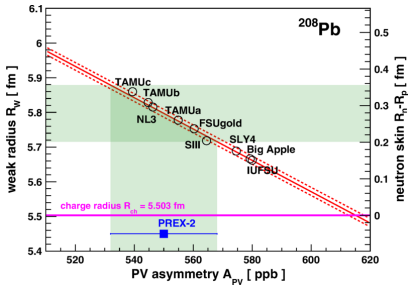
$$\mathcal{A}_{\text{cor}} = \mathcal{A}_{\text{raw}} - \sum_i \beta_i \Delta x_i$$

$$\mathcal{A}_{\text{PV}} = \frac{\mathcal{A}_{\text{cor}}/\mathcal{P} - \sum_i \mathcal{A}_i f_i}{1 - \sum_i f_i}$$

\mathcal{A} (ppb)	PREX-II	CREX
\mathcal{A}_{raw}	431.64 ± 44.01	2106 ± 178.9
\mathcal{A}_{cor}	492.02 ± 13.52	2080.3 ± 83.8
\mathcal{A}_{PV}	$549.4 \pm 16.1_{\text{stat}} \pm 8.1_{\text{syst}}$	$2412.3 \pm 106.1_{\text{stat}} \pm 38.7_{\text{syst}}$
Unblinded \mathcal{A}_{PV}	$550.0 \pm 16_{\text{stat}} \pm 8_{\text{syst}}$	$2668 \pm 106_{\text{stat}} \pm 40_{\text{syst}}$

Final Number: R_{skin}

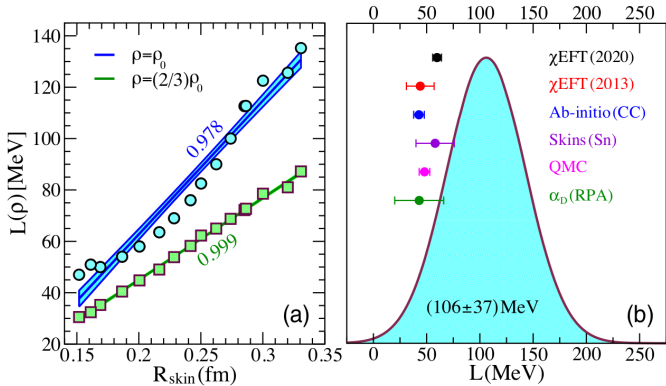
PRL 126, 172502



Exp	PREX-II	CREX
Target	^{208}Pb	^{48}Ca
$\langle Q^2 \rangle$ (GeV 2)	0.00616 ± 0.00005	0.0297 ± 0.0002
$\langle A_{\text{PV}} \rangle$ (ppb)	$550 \pm 16_{\text{stat}} \pm 8_{\text{syst}}$	$2668 \pm 106_{\text{stat}} \pm 40_{\text{syst}}$
F_W	$0.368 \pm 0.013_{\text{exp}} \pm 0.001_{\text{theo}}$	$0.1304 \pm 0.0052_{\text{stat}} \pm 0.0020_{\text{syst}}$
$F_{ch} - F_W$	$0.041 \pm 0.013_{\text{exp}} \pm 0.001_{\text{theo}}$	$0.0277 \pm 0.0052_{\text{stat}} \pm 0.0020_{\text{syst}}$
R_W (fm)	$5.795 \pm 0.082_{\text{exp}} \pm 0.013_{\text{theo}}$	$3.640 \pm 0.026_{\text{exp}} \pm 0.023_{\text{theo}}$
$R_n - R_p$ (fm)	$0.278 \pm 0.078_{\text{exp}} \pm 0.012_{\text{theo}}$	$0.121 \pm 0.026_{\text{exp}} \pm 0.024_{\text{theo}}$

Final Number: L

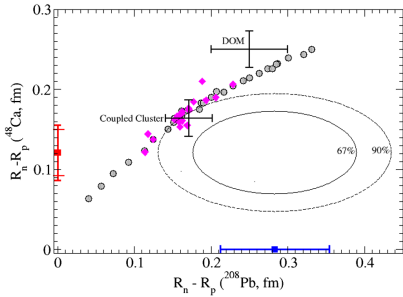
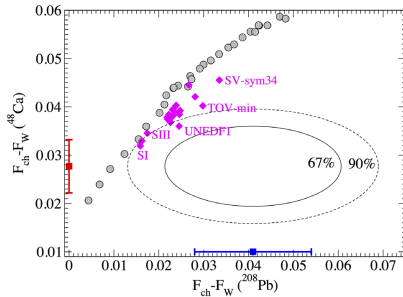
PRL 126, 172503



$$L(\rho_0) = 106 \pm 37 \text{ MeV} \quad L(\rho_1) = 71.5 \pm 22.6 \text{ MeV}$$

Physical Implications: Nuclear Theory

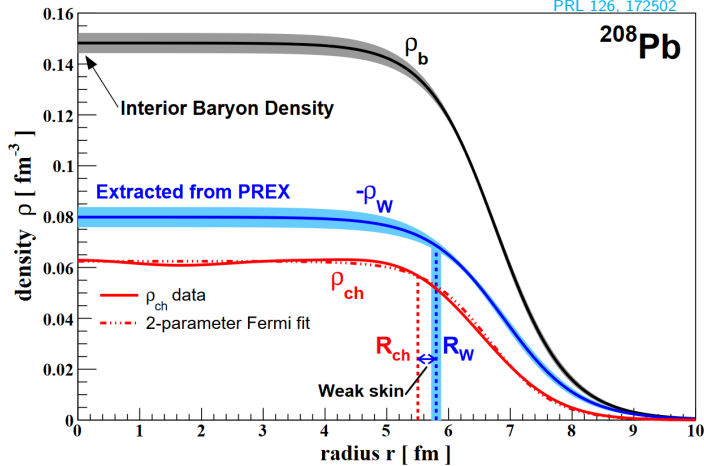
PRL 129, 042501



- Our results will guide the development of nuclear theories
- Only a few models' predictions match with both measurements simultaneously
- More work, from both experimental and theoretical sides, are needed to accommodate the difference between them

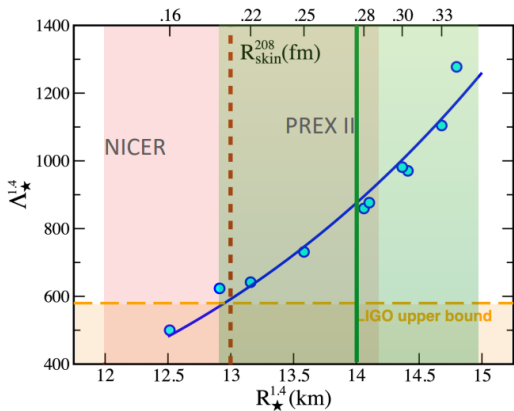
Physical Implications: Nuclear Saturation Density

PRL 126, 172502



- Interior baryon density: $\rho_b = 0.1482 \pm 0.0040 \text{ fm}^{-3}$
- Nuclear saturation density: $\rho_0 = 0.1510 \pm 0.0059 \text{ fm}^{-3}$

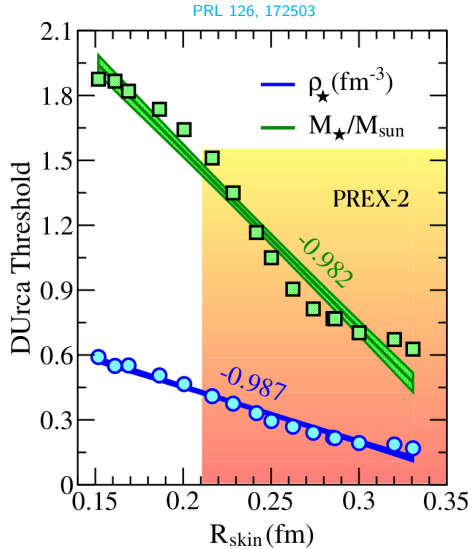
Physical Implications: Size of a Neutron Star



PREX-II result

- supports a large neutron star radius
- is consistent with the NICER result
- is in mild tension with the LIGO observation

Physical Implications: The Direct Urca Process in Neutron Stars



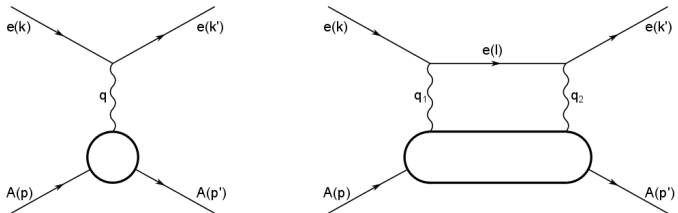
- PREX-II R_{skin} supports a lower threshold density:

$$\rho_{\star} \approx 0.24 \text{ fm}^{-3}$$

$$M_{\star} \approx 0.85 M_{\odot}$$

Transverse Asymmetry

Introduction

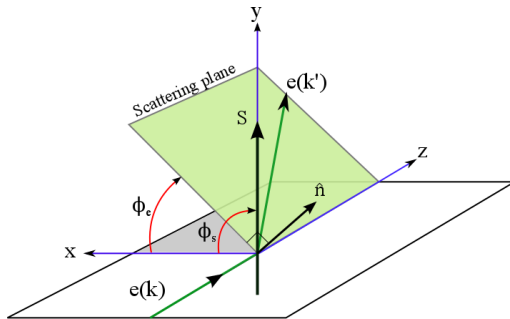


Transverse Asymmetry (Beam Normal Single Spin Asymmetry):

$$A_n = \frac{\sigma_{\uparrow} - \sigma_{\downarrow}}{\sigma_{\uparrow} + \sigma_{\downarrow}} \approx 0 + \frac{2\text{Im}(T_{2\gamma} \cdot T_{1\gamma}^*)}{|T_{1\gamma}|^2}$$

- A_n is 0 under Born approximation
- A_n is sensitive to Two Photon Exchange (TPE) interaction
- A_n is a systematic uncertainty in the A_{PV} measurement for PREX-II/CREX

How to Measure Transverse Asymmetry

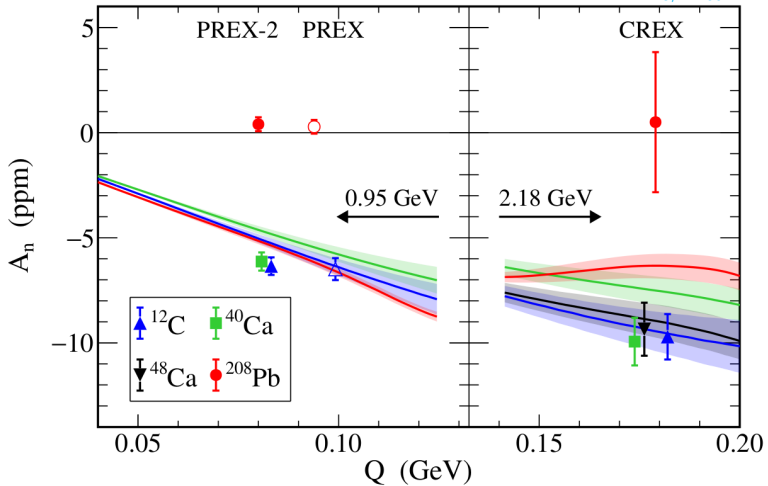


$$\mathcal{A}_{\text{meas}}(\phi_e) = \mathcal{A}_n(\vec{S}_e \cdot \hat{\mathbf{n}}) = \mathcal{A}_n |\vec{S}_e| \sin(\phi_e - \phi_s)$$

- $\hat{\mathbf{n}} \equiv \frac{(\vec{k} \times \vec{k}')}{|\vec{k} \times \vec{k}'|}$: normal direction of the scattering plane
- Azimuthal angle (ϕ_e) dependent
- Choose ϕ_s to be: 0° (horizontal) or 90° (**vertical**)

AT Result

PRL 128, 142501



- A_n for $\text{Pb}208$ is consistently 0 at different Q^2 values
- First measurement of a new nucleus: $\text{Ca}40$

Summary

Parity Violating Asymmetry measurement

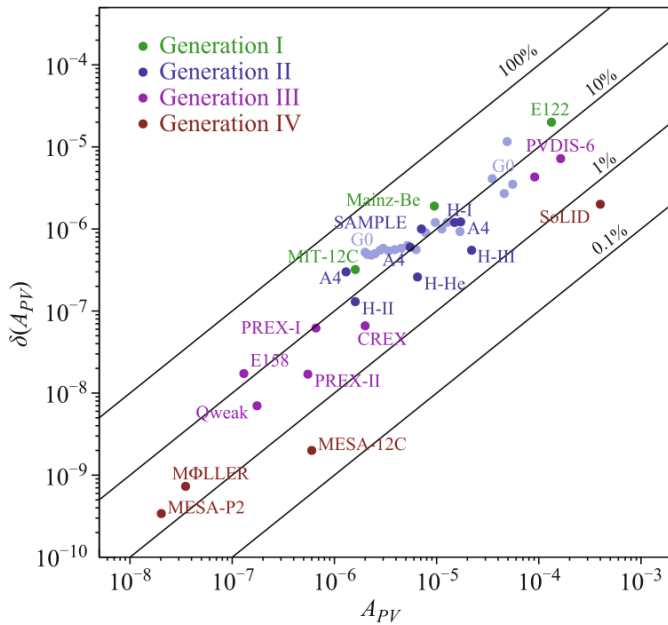
- Precise measurements of the neutron skin thicknesses of Pb208 and Ca48 (the first time)
- Both measurements are statistics limited
- **Constrain nuclear models and the density dependence of the symmetry energy (L)**

Transverse Asymmetry measurement

- Theory calculations agree with measurements for light nuclei
- **Transverse asymmetry is found to be consistent with 0 for Pb208 at all Q**

Backup

History of PVES



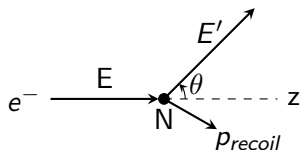
Form Factors

$$\begin{aligned}\mathcal{A}_{PV} &= \frac{\frac{d\sigma^R}{d\Omega} - \frac{d\sigma^L}{d\Omega}}{\frac{d\sigma^R}{d\Omega} + \frac{d\sigma^L}{d\Omega}} = \frac{|\mathcal{M}^R|^2 - |\mathcal{M}^L|^2}{|\mathcal{M}^R|^2 + |\mathcal{M}^L|^2} \\ &\approx \frac{\mathcal{M}_Z^R - \mathcal{M}_Z^L}{\mathcal{M}_\gamma} \propto \frac{\frac{d\sigma_{\text{weak}}}{d\Omega}}{\frac{d\sigma_{\text{E+M}}}{d\Omega}} \quad (\text{for low } Q^2) \\ &\approx \frac{G_F Q^2}{4\pi\alpha\sqrt{2}} \frac{Q_{wk}}{Z} \frac{F_{wk}(Q^2)}{F_{ch}(Q^2)}\end{aligned}$$

where: $\mathcal{M}^{R,L} = \mathcal{M}_\gamma + \mathcal{M}_Z^{R,L}$ ($\mathcal{M}_\gamma \gg \mathcal{M}_Z$) and

$$F(Q^2) = \int d^3r \frac{\sin(Qr)}{Qr} \rho(r)$$

Dynamics



$$E' = \frac{ME}{M + E(1 - \cos \theta)}$$

where M is the mass of the target nucleus

- with very small scattering angle $\theta \sim 5^\circ$, $E' \approx E$, quasi-elastic scattering
- $Q^2 = -q^2 = -[(E - E')^2 - (\vec{p} - \vec{p}')^2] = 2EE'(1 - \cos \theta)$

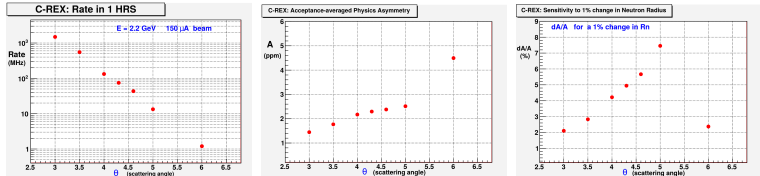
Parameters

	PREX-II	CREX
Energy (GeV)	0.95	2.18
Beam current (μ A)	50-85	100-150
Polarization (%)	89.7	87.1
Scattering angle θ (deg)	4.7	4.5
Q^2 (GeV 2)	0.00616	0.0297
Scattering rate (MHz/ μ A/arm)	\sim 30	\sim 0.2
Collected charge (C)	114	412

Figure-of-Merit (FOM)

$$\text{FOM} = R \times \mathcal{A}^2 \times \epsilon^2$$

- R : scattering rate
- \mathcal{A} : asymmetry
- $\epsilon = \frac{d\mathcal{A}/\mathcal{A}}{dR_n/R_n}$: sensitivity of the asymmetry w.r.t. neutron radius



Asymmetry of ^{208}Pb

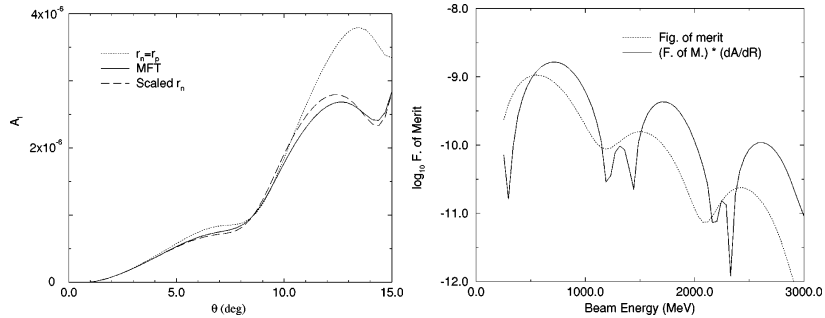


Figure: Parity-Violating asymmetry for ^{208}Pb . Left: $E = 850 \text{ GeV}$; Right: $\theta = 6 \text{ deg}$

Neutron Skin Thickness of ^{48}Ca

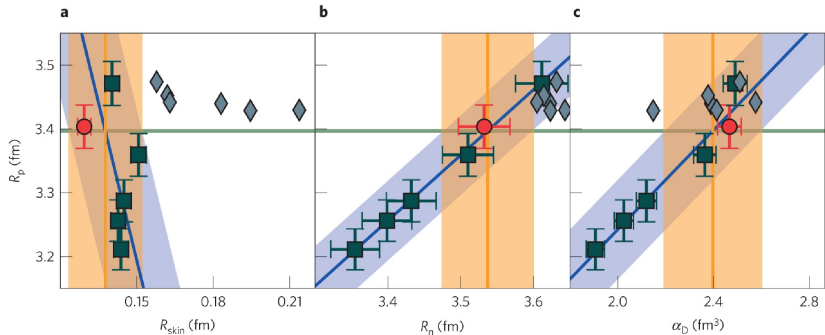


Figure: Ab-initio calculation of the neutron skin thickness of ^{48}Ca . From left to right, neutron skin thickness (a), neutron radius (b) and electric dipole polarizability (c) of ^{48}Ca are plotted versus its proton radius. The ab-initio predictions are shown as red circles and dark squares, while DFT results are represented by gray diamonds. The blue line represents a linear fit to ab-initio predictions. The horizontal green line marks the experimental value of R_p , whose intersection with the blue line.
nphys3529

Neutron Skin Thickness of ^{208}Pb

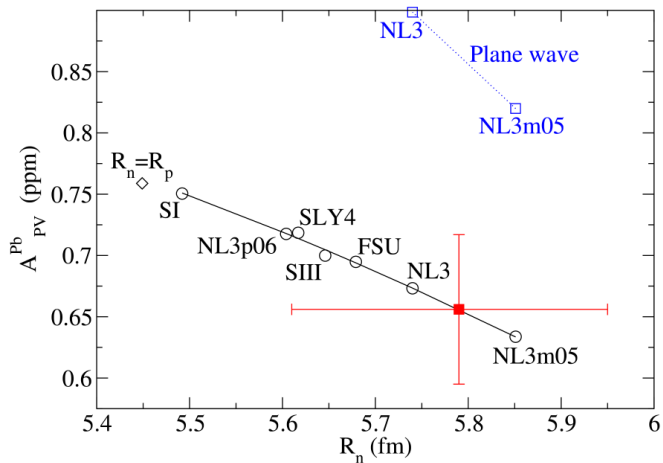
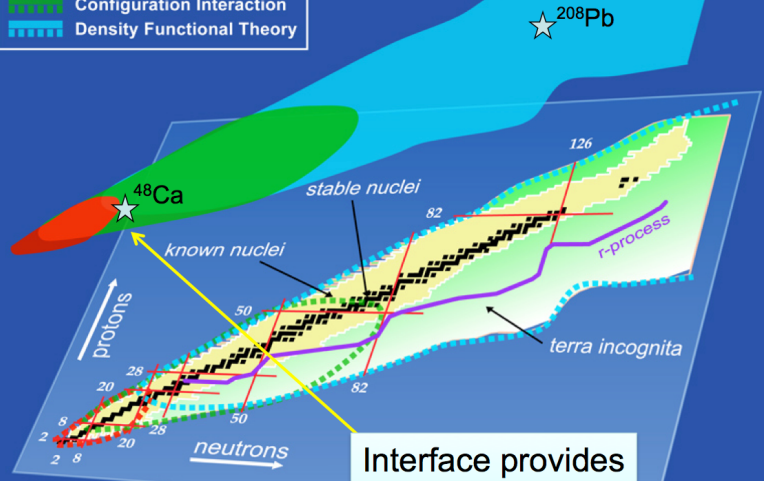


Figure: PREX-I result (red square). [PhysRevLett.108.112502](https://doi.org/10.1103/PhysRevLett.108.112502)

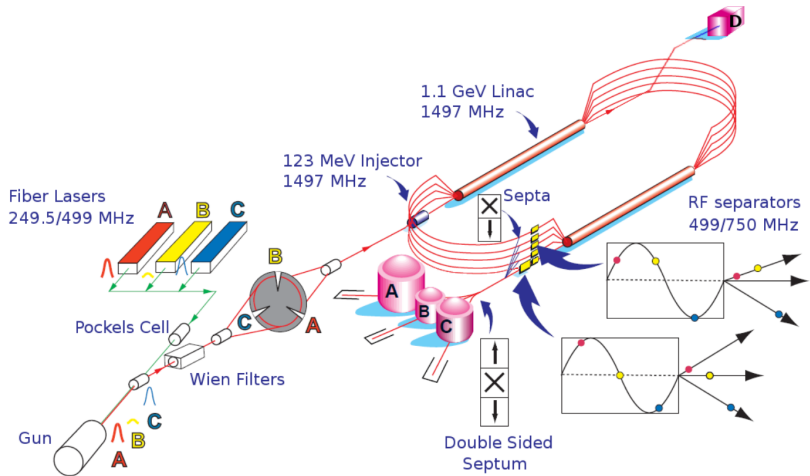
Nuclear Landscape

Nuclear Landscape

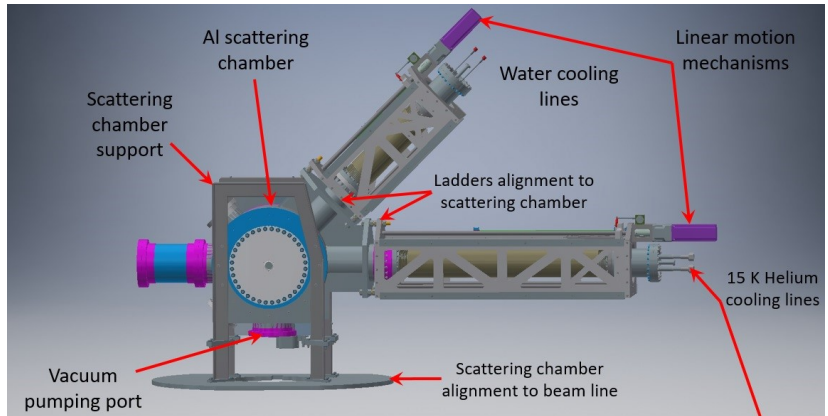
- Ab initio
- Configuration Interaction
- Density Functional Theory



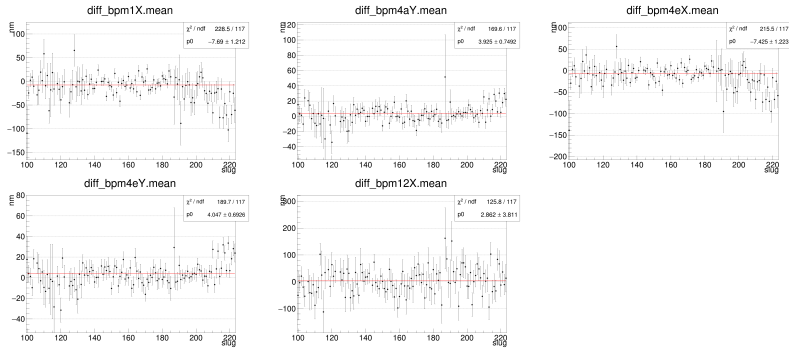
CEBAF



Target Chamber



Helicity Correlated Beam Asymmetry (HCBA)

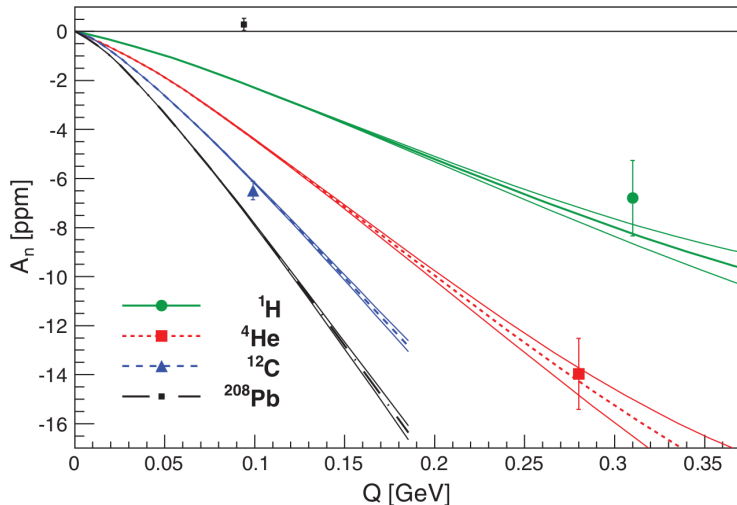


$$e(\rho, \beta) = e(\rho, 0) + S(\rho)\beta^2 + O(\beta^4)$$

$S(\rho)$ is what we call symmetry energy

PREX-I Result

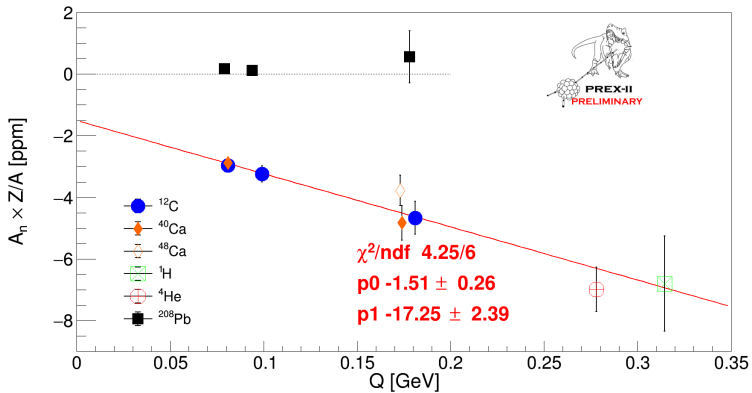
PREX-I PRL 109, 192501 (2012)



- Theoretical predictions match A_n measurements of light nuclei

Weibin Zhai To everyone's surprise, A_n for Pb^{208} was measured to be 0 59

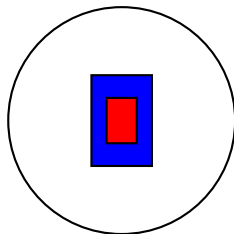
Phenomenological Fit



- For light nuclei, the linear fit of $A_n \times Z/A$ vs Q looks good
- Observe that it has a non-zero offset

Collimator Power

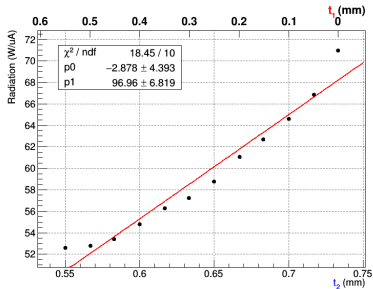
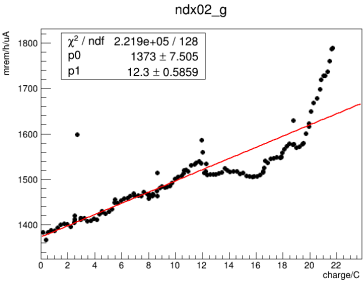
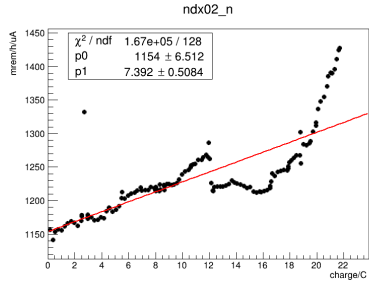
- Collimator is key component in these experiments, we need to make sure radiation deposit on collimator is under control
- The radiation power on collimator tells us the quality of target



central thickness: t_1
outer thickness: t_2

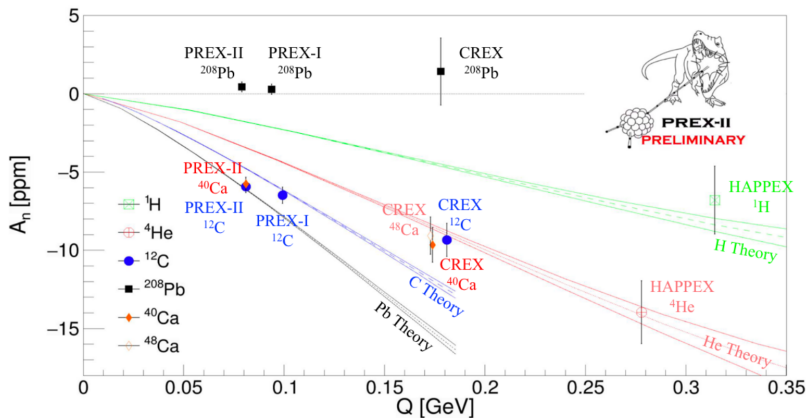
t_1 (mm)	t_2 (mm)	Power/Current (W/ μ A)
0.55	0.550	52.6172
0.45	0.583	53.4176
0.35	0.617	56.2972
0.25	0.650	58.7556
0.15	0.683	62.6694
0.05	0.717	66.8324

Collimator Power



- Simulation result is consistent with experimental data: radiation increases along charge accumulation (target degradation)

All Hall A Measurements



- A_n for Pb^{208} was found to be 0 at three different Q values
- For light nuclei, theoretical calculations follow the observed experimental measurements and trends

$$G_{E,M}^{p,\gamma} = \frac{2}{3}G_{E,M}^u - \frac{1}{3}G_{E,M}^d - \frac{1}{3}G_{E,M}^s$$

$$G_{E,M}^{n,\gamma} = \frac{2}{3}G_{E,M}^d - \frac{1}{3}G_{E,M}^u - \frac{1}{3}G_{E,M}^s$$

$$G_{E,M}^{n,Z^0} = \left(\frac{1}{4} - \sin^2 \theta_W \right) G_{E,M}^u + \left(-\frac{1}{4} + \frac{1}{3} \sin^2 \theta_W \right) \times (G_{E,M}^d + G_{E,M}^s)$$

Radius

$$R_n - R_p = \left[1 + \frac{ZQ_p}{NQ_n} \right] (R_{wk} - R_{ch})$$

$$R_{ch} = 5.503 \text{ fm}$$

$$R_p = \sqrt{R_{ch}^2 - r_p^2} = 5.432 \text{ fm}$$

$$R_n - R_p = 0.278 \pm 0.078 \text{ fm}$$

Two-Parameter Fermi Function

$$\rho_w(r, c, a) = \rho_w^0 \frac{\sinh(c/a)}{\cosh(r/a) + \cosh(c/a)}$$

$$\rho_w^0 = \frac{3Q_w}{4\pi c(c^2 + \pi^2 a^2)}$$

$$R_w^2 = \frac{1}{Q_w} \int r^2 \rho_w(r) d^3 r = \frac{3}{5} c^2 + \frac{7}{5} (\pi a)^2$$

$$\rho_w^0 = \frac{27Q_w}{4\pi(5R_w^2 - 4\pi^2 a^2) \sqrt{15R_w^2 - 21\pi^2 a^2}}$$

$$R_w = 5.795 \pm 0.082 \text{ fm}$$

$$a = 0.605 \pm 0.025 \text{ fm from theory}$$

$$Q_w = NQ_w^n + ZQ_w^p = -118.78$$

$$\rho_w^0 = 0.080 \pm 0.004 \text{ fm}^{-3}$$

$$\rho_b^0 = \frac{-\rho_w^0}{q_n} + \left(1 - \frac{q_p}{q_n}\right) \rho_c^0$$